



Published in final edited form as:

Circulation. 2015 January 13; 131(2): 190–199. doi:10.1161/CIRCULATIONAHA.114.013339.

Restoration of Impaired Endothelial MEF2 Function Rescues Pulmonary Arterial Hypertension

Jongmin Kim, Ph.D.^{1,2,*}, Cheol Hwangbo, Ph.D.^{1,*}, Xiaoyue Hu, B.A.¹, Yujung Kang, Ph.D.^{1,**}, Irinna Papangeli, Ph.D.¹, Devi Mehrotra, B.A.¹, Hyekyung Park, M.S.¹, Hyekyung Ju, M.S.¹, Danielle L. McLean, Ph.D.¹, Suzy A. Comhair, Ph.D.³, Serpil C. Erzurum, M.D.³, and Hyung J. Chun, M.D.¹

¹Yale Cardiovascular Research Center, Section of Cardiovascular Medicine, Yale University School of Medicine, New Haven, CT

²Department of Life Systems, Sookmyung Women's University, Seoul 140-742, Korea

³Department of Pathobiology, The Lerner Institute, The Cleveland Clinic Foundation, Cleveland, OH

Abstract

Background—Pulmonary arterial hypertension (PAH) is a progressive disease of the pulmonary arterioles, characterized by increased pulmonary arterial pressure and right ventricular failure. The etiology of PAH is complex, but aberrant proliferation of the pulmonary artery endothelial cells (PAECs) and pulmonary artery smooth muscle cells (PASMCs) is thought to play an important role in its pathogenesis. Understanding the mechanisms of transcriptional gene regulation involved in pulmonary vascular homeostasis can provide key insights into potential therapeutic strategies.

Methods and Results—We demonstrate that the activity of the transcription factor myocyte enhancer factor 2 (MEF2) is significantly impaired in the PAECs derived from subjects with PAH. We identified MEF2 as the key cis-acting factor that regulates expression of a number of transcriptional targets involved in pulmonary vascular homeostasis, including microRNAs 424 and 503, connexins 37, connexin 40, Kr ppe1 Like Factor 2 (KLF2) and KLF4, which were found to be significantly decreased in PAH PAECs. The impaired MEF2 activity in PAH PAECs was mediated by excess nuclear accumulation of two class IIa histone deacetylases (HDACs) that inhibit its function, namely HDAC4 and HDAC5. Selective, pharmacologic inhibition of class IIa HDACs led to restoration of MEF2 activity in PAECs, as demonstrated by increased expression of its transcriptional targets, decreased cell migration and proliferation, and rescue of experimental pulmonary hypertension (PH) models.

Conclusions—Our results demonstrate that strategies to augment MEF2 activity holds potential therapeutic value in PAH. Moreover, we identify selective HDAC IIa inhibition as a viable

Correspondence: Hyung J. Chun, MD, Yale University School of Medicine, Section of Cardiovascular Medicine, 300 George Street, Room 770H, New Haven, CT 06511, Phone: 203-737-6389, Fax: 203-737-6118, hyung.chun@yale.edu.

** Current address: R&D Center, Vieworks Co., Ltd., Gyeonggi-do, Korea

* contributed equally

Disclosures: None.

alternative approach to avoid the potential adverse effects of broad spectrum HDAC inhibition in PAH.

Keywords

pulmonary hypertension; endothelial function; transcriptional regulation

Introduction

Pulmonary arterial hypertension (PAH) involves abnormal proliferation of pulmonary vascular cells, resulting in pulmonary arterial remodeling and obliteration of the pulmonary vascular lumen. Ultimate clinical outcomes include increased pulmonary vascular resistance and right ventricular (RV) failure. Recent studies have extended our understanding of the pathogenesis of disease, including identification of growth factors/cytokines, transcription factors, and microRNAs that play key roles in the disease progression.^{1, 2} However, despite these advancements, there is a clear need for better understanding of the mechanisms of the disease process, given the persistently high mortality rates in this patient population.³

Many cell types are known to play important roles in the overall pathogenesis of PAH, including PAECs, PASMCs, fibroblasts, and pericytes.¹ With respect to PAECs, their dysregulated proliferation, especially in the plexiform lesions that are present in up to 80% of the patient population, has been extensively demonstrated in histopathological studies.⁴ Moreover, recent studies have identified a number of secreted factors from PAECs that likely have key roles in aberrant cellular proliferation, including FGF2, IL-6 and endothelin-1.⁵⁻⁷ These signaling perturbations likely have both autocrine and paracrine consequences, where these endothelial factors induce proliferation, migration, and vascular remodeling and target PAECs, PASMCs and pericytes in the pathogenesis of PAH.

Despite the increased knowledge of changes in endothelial gene expression in PAH, the transcriptional mechanisms that regulate the expression of these factors remain poorly understood. Here we identify a novel, key role for the transcription factor MEF2 in maintenance of pulmonary vascular homeostasis. We found that MEF2 transcriptional activity is significantly decreased in PAH PAECs, and it functions as a cis-acting transcription factor that regulates the expression of miR-424 and miR-503, two miRNAs involved in maintenance of pulmonary vascular homeostasis.⁸ Moreover, we found a significant decrease in expression of a multitude of MEF2 transcriptional targets. The impaired MEF2 activity in PAH PAECs was associated with increased nuclear accumulation of two class IIa histone deacetylases (HDACs), namely HDAC4 and HDAC5. Augmenting MEF2 activity by selective inhibition of class IIa HDACs can rescue experimental PAH models, without any evidence of worsening RV remodeling, fibrosis, or coronary artery endothelial apoptosis, which had been previously associated with non-selective HDAC inhibition.⁹ Our findings provide significant advancement of the mechanisms of transcriptional regulation that are involved in PAH, and also provide novel critical insights into the controversies surrounding the potential use of HDAC inhibition in PAH,¹⁰⁻¹³ where conflicting data has shrouded the promise of targeting this class of molecules as a therapeutic strategy.

Methods

An extended Methods is available in the online-only Data Supplement.

Human samples

The study was approved by the Cleveland Clinic and the Yale University School of Medicine Institutional Review Boards, and written informed consent was obtained from all participating individuals. The clinical information for the patients from whom the cells were isolated are listed in Sup. Table 1.

Animal studies

Animal experiments performed in this study were approved by the Institutional Animal Care and Use Committee of Yale University.

Cell culture and reagents

We isolated PAECs from normal and PAH explanted donor lungs, as described previously.^{14, 15} We obtained additional control PAECs from Lonza. PAECs from seven control subjects, seven subjects with IPAH and three subjects with FPAH were studied. In brief, human pulmonary arteries were dissected from the lungs to the distal small arterioles, and PAECs were harvested from the isolated pulmonary arterial tree. PAECs were grown in EBM-2 basal medium supplemented with EGM-2 (Lonza) on fibronectin-coated plates. Cells were passaged at 70–80% confluency, and primary cultures of passages 3 to 7 were used in experiments. All apelin stimulations were done using apelin-13 peptide at 1 μ M (Sigma). TSA (Sigma) and MC1568 (Selleck Chemicals and DC Chemicals) were dissolved in DMSO (Sigma) and used at the indicated doses.

Immunohistochemistry of lung sections

PAH and control donor lung samples were obtained from the National Disease Research Interchange (NDRI). Human and rat lung tissues were fixed and stained as previously described.⁸ Standard methods (Trichrome Stain, Sigma) were used to stain for collagen in cardiac sections.

Immunofluorescence

For the apelin effect on HDAC4/5 translocation, PAECs plated on glass bottom culture dish (Mat-Tek) were transfected with GFP-tagged HDAC4 and HDAC5 expression vectors for 24 hours. Cells were imaged using a Nikon Eclipse Ti confocal microscopy before and after treatment with apelin 13 (1 μ M for 1 h at 37°C).

Pulmonary hypertension animal models

Male Sprague Dawley rats (200–250 g; Charles River Laboratories) were subcutaneously injected with monocrotaline (Sigma) (60 mg per kg body weight) for the MCT model. For the SUGEN model, SU-5416 (Sigma) was resuspended in DMSO (Sigma) and injected subcutaneously (20 mg per kg body weight). Rats were subsequently exposed to hypoxia (10% FiO₂) for 2 weeks. Rats were given intraperitoneal administration of either the vehicle

(DMSO) or MC1568 (Sellek Chemicals and DC Chemicals) (50 mg per kg body weight) daily.

Hemodynamic and morphometric analyses

Right ventricular systolic pressure (RVSP) measurements were performed at the designated time point under isoflurane anesthesia by inserting a catheter (Millar Instruments) into the right jugular vein as described previously.⁸ Six to eight animals were tested per experimental group based on our previous studies. Lungs were perfused with normal saline and fixed in 4% paraformaldehyde overnight for immunohistochemistry or snap frozen in liquid nitrogen for protein and RNA analyses. Hearts were dissected and weighed for calculation of the right ventricle (RV) to the left ventricle (LV) plus septum weight ratio (weight of the RV divided by the weight of the LV + septum). The same full section in the midportion of the left lung parallel to the hilum was used and embedded in the same manner for lung morphometric analyses. Pulmonary artery muscularization was assessed at $\times 200$ magnification after staining for vWF and SMA by calculating the ratio of the number of muscularized peripheral pulmonary arteries to the number of total peripheral pulmonary vessels (with diameters less than 75 μm) in five random fields per lung (with each field at $\times 200$ magnification). Pulmonary arteries with proliferating cells were assessed in PCNA stained lung sections. Vessels with one or more PCNA stained cells were considered to be PCNA positive. All measurements were carried out by investigators blinded to the experimental condition.

Statistical analyses

All experiments were performed in triplicate (unless otherwise specified) from at least three independent experiments, and data shown are the means \pm s.e.m. When only two groups were compared, statistical differences were assessed with unpaired two-tailed Student's *t* test. Otherwise, statistical significance was determined using one-way analysis of variance followed by Bonferroni's multiple comparison test. Relationships between variables were determined by the Pearson correlation coefficient. $P < 0.05$ was considered statistically significant.

Results

MEF2 is a key transcription factor that regulates miR-424 and miR-503

We sought to identify the transcriptional machinery that regulates expression of miR-424 and miR-503 (miR-424/503), which were recently found to be the link in the disruption of the apelin-FGF signaling axis in PAH PAECs.⁸ *In silico* analysis of the putative miR-424/503 promoter region (mapper.chip.org) identified at least two highly conserved MEF2 binding sites (Sup. Fig. 1). We found that knockdown of *MEF2A* and *MEF2C*, which are the MEF2 isoforms known to be highly expressed in endothelial cells, in human PAECs led to a significant decrease in miR-424 and miR-503 expression (Fig. 1A); chromatin immunoprecipitation (ChIP) assays confirmed binding of MEF2 to the two conserved MEF2 binding sites in the miR-424/503 promoter in PAECs (Fig. 1B). MiR-424/503 promoter based luciferase reporter construct was significantly induced by co-transfection with either

MEF2A or MEF2C; this effect was abrogated by mutagenesis of the MEF2 binding sites (Fig. 1C).

We next investigated whether MEF2 is also the key mediator of apelin induced miR-424 and miR-503 expression. Stimulation of PAECs with apelin, in conjunction with knockdown of *MEF2A* and *MEF2C*, led to abrogation of apelin mediated activation of the miR-424/503 promoter (Fig. 1D). Moreover, the miR-424/503 promoter based reporter containing mutagenized MEF2 binding sites also failed to respond to apelin (Sup. Fig. 2). ChIP assay showed that siRNA mediated knockdown of *APLN* in PAECs resulted in a marked reduction in MEF2 binding to the miR-424/503 promoter (Fig. 1E).

MEF2 transcriptional activity is impaired in PAH PAECs

To further corroborate these findings to the PAH context, we evaluated whether overall MEF2 activity may be compromised in PAH PAECs. We found that the total transcript levels of MEF2A and MEF2C were not significantly different between control and PAH PAECs, suggesting that the expression levels of MEF2 was not affected in PAH PAECs (Sup. Fig. 3). However, the baseline activity of two MEF2 responsive reporters, derived from the miR-424/503 promoter and the Kr ppe1 Like Factor 2 (KLF2) promoter,¹⁶ were significantly lower in PAH PAECs compared to controls (Fig. 1F and 1G). Moreover, we found that stimulation of PAH PAECs with apelin led to a significant augmentation of the MEF2 reporter activity in PAH PAECs tested, demonstrating that the compromised MEF2 activity in these cells can be augmented by apelin (Fig. 1H).

Increased nuclear localization of HDAC4 and HDAC5 inhibit MEF2 function in PAH PAECs

MEF2 is known to be regulated by multiple mechanisms, one of which is its inhibition by class IIa histone deacetylases (HDACs).^{17, 18} Class IIa HDACs, comprised of HDAC4, HDAC5, HDAC7, and HDAC9, are the only HDACs known to bind to MEF2. Interestingly, only HDAC4 and HDAC5 protein levels were previously found to be increased in the lungs of PAH patients.¹² Moreover, apelin mediated regulation of MEF2 activity was found to involve phosphorylation and cytoplasmic translocation of HDAC4 and HDAC5.¹⁹ Based on this knowledge, we carried out a series of studies to evaluate the potential role of specifically targeting this class of HDACs in PAH. We found that PAH PAECs had a significantly higher fraction of transfected HDAC4 and HDAC5 that localized to the nucleus, compared to control PAECs (Fig. 2A). This finding was consistently observed in PAECs derived from three independent PAH subjects compared to control PAECs. Moreover, we found that stimulation of PAH PAECs with apelin led to robust cytoplasmic translocation of both HDAC4 and HDAC5 (Fig. 2B), as well as marked increase in phosphorylation of HDAC4 and HDAC5 (Fig. 2C), which is known to be closely associated with their cytoplasmic translocation.^{20, 21}

Inhibition of class IIa HDACs augments MEF2 transcriptional activity in PAECs

We next determined whether inhibition of HDAC4 and HDAC5 can augment MEF2 activity in PAECs. Selective inhibition of HDAC4 and HDAC5 by siRNA mediated knockdown in PAH PAECs led to a significant increase in miR-424 and miR-503 expression in these cells (Fig. 3A). Moreover, our previously described MEF2 transcriptional targets with possible

roles in the pathogenesis of PAH, including connexin 37 (Cx37), connexin 40 (Cx40), and KLF2,¹⁹ as well as the related, MEF2 regulated KLF4 (Sup. Table 2), were also significantly upregulated by *HDAC4* and *HDAC5* knockdown in PAH PAECs (Fig. 3A). In addition, we found in PAH PAECs significantly decreased transcript levels of Cx37, Cx40, KLF2 and KLF4 compared to controls (Fig. 3B), providing further evidence that MEF2 transcriptional activity is reduced in these cells. We also evaluated the expression of two of these targets, namely Cx37 and Cx40, in the lung tissue of PAH subject and control. We found that the expression level of both Cx37 and Cx40 was significantly decreased in the endothelial layer of lung from PAH subject compared to control (Fig. 3C).

Next, we determined the efficacy of a pharmacologic HDAC class IIa specific inhibitor, MC1568, on MEF2 target expression. MC1568 has been demonstrated to have selective inhibition of class IIa HDACs, without affecting other HDAC classes, at least in part by inducing degradation of HDAC4 and HDAC5.^{22, 23} We found that treatment of PAECs with MC1568 led to a significant decrease in the protein levels of HDAC4 and HDAC5 (Sup. Fig. 4). Treatment of PAH PAECs with MC1568 resulted in significantly increased expression of miR-424, miR-503, Cx37, Cx40, and KLF2 (Fig. 3D). Moreover, we found that treatment of PAH PAECs with MC1568 leads to a significant downregulation of FGF2, which was previously found to be targeted by miR-424 and miR-503, and aberrantly increased in PAH PAECs (Sup. Fig. 5).^{6, 8} MC1568 treatment also led to significant reduction of PAH PAEC proliferation (Fig. 3E) and migration (Fig. 3F).

Pharmacological inhibition of class IIa HDACs results in rescue of experimental PH models

Given our in vitro findings demonstrating the effects of MC1568, we tested two experimental PH models (monocrotaline (MCT) and SU-5416/hypoxia (SUGEN)) to determine the efficacy of MC1568 in reversing established PH in rats (Sup. Fig. 6). Measurement of the right ventricular systolic pressures (RVSP) demonstrated a significant decrease in MC1568 administered rats compared to controls in both the MCT and the SUGEN models (Fig. 4A). We also found a significant reduction in the RV to left ventricle + septum (LV+S) weight ratios in the MC1568 groups (Fig. 4B). Morphometric lung studies demonstrated a significantly decreased number of muscularized arterioles in the MC1568 groups (Fig. 4C). Moreover, PCNA-positive proliferating vascular cells were significantly fewer in MC1568 treated groups compared to control groups (Fig. 4D). The number of obliterated lumens was also significantly fewer in the MC1568 treated lungs compared to the control group in the SUGEN model (Fig. 4E). At the molecular level, MC1568 treatment also led to a significant increase in expression levels of rno-mir-322 (rat homolog of hsa-miR-424) and rno-mir-503 (Fig. 4F), as well as other MEF2 transcriptional targets, although some of these did not reach statistical significance in the MCT model (Sup. Fig. 7). Lastly, expression of FGF2 was significantly decreased in the lungs of MC1568 administered rats (Fig. 4G).

Selective class IIa HDAC inhibition avoids the adverse RV effects of global HDAC inhibition

We next evaluated whether selective HDAC class IIa inhibition can potentially avoid the deleterious cardiac effects seen with broader HDAC inhibition.⁹ Unlike what was described with trichostatin A (TSA), we found no evidence of myocardial fibrosis in rats receiving MC1568 in both the MCT and SUGEN groups (Fig. 5A). Moreover, we found that treatment of human coronary artery endothelial cells with TSA, a broad spectrum HDAC inhibitor, lead to marked induction of cellular apoptosis as assessed by caspase 3 cleavage, while MC1568 treatment did not result in caspase activation even at a higher concentration (Fig. 5B). Lastly, gross histological analyses of the right ventricle demonstrated that the MC1568 group had marked protection from the RV dilatation and remodeling that was observed in the control group (Fig. 5C). The RV mass was markedly smaller in the rats treated with MC1568 in both the MCT and the SUGEN groups, as well as the RV to total body weight ratios (Fig. 5D).

Discussion

Here we report the key observation that MEF2, involved in transcriptional regulation of a number of endothelial genes that mediate vascular homeostasis, is impaired in PAH PAECs. Moreover, similar to our recent findings in the broad endothelial context, we found that apelin can robustly augment MEF2 activity in PAECs, through a mechanism that involves phosphorylation and cytoplasmic translocation of two class IIa HDACs, namely HDAC4 and HDAC5. Apelin has been identified as a key component of pulmonary vascular homeostasis, that is implicated as a downstream target of BMP signaling.^{8, 24–27} We found that selective pharmacologic inhibition of class IIa HDACs using MC1568 induced expression of multiple MEF2 targets in PAECs, including miR-424, miR-503, Cx37, Cx40, KLF2 and KLF4. Most importantly, we found that selective class IIa HDAC inhibition rescues two independent experimental PH models in rats (Fig. 5E for schematic).

Two MEF2 factors are known to be highly expressed in the endothelial cells: MEF2A and MEF2C.^{28, 29} Mice with genetic deletion of these genes succumb to either embryonic (MEF2C) or early postnatal (MEF2A) lethality,^{30, 31} hence studies of these genes in mature vascular function have been limited. Interestingly, recent evaluation of the retinal vasculature of a conditional, endothelial cell specific MEF2C knockout mouse demonstrated enhanced vascular growth and decreased EC apoptosis.³² Moreover, expression of FGF2 was found to be significantly increased in ECs subjected to MEF2C knockdown. Overall, these findings suggest that MEF2 is a key endothelial homeostatic transcription factor that likely regulates a multitude of endothelial transcripts, including Cx37/40, KLF2/4, and miR-424/503, to maintain vascular quiescence. In addition, our results support the important role of our previously defined apelin-miR-424/503-FGF2/FGFR1 signaling axis in PAH,⁸ with the demonstration that disruption of apelin or miR-424/503 in PAH PAECs likely is a key contributor to the aberrant increase in FGF2 levels seen in PAH subjects.^{6, 33}

A number of recent studies have demonstrated the potential therapeutic efficacy of using broad spectrum HDAC inhibitors in experimental models of PH.^{10, 12, 34} However, other studies have raised concerns regarding the use of broad spectrum HDAC inhibitors, where

worsening of RV function and induction of RV capillary death were observed,^{9, 11} and TSA failed to improve RVSP or RV function in the SUGEN model of PH.¹³ Despite the unresolved controversies highlighted by these studies, HDAC inhibition to treat PAH may be an attractive therapeutic strategy, given that two such agents (vorinostat and romidepsin) are currently in use for patients with cutaneous T cell lymphoma.³⁵ Unfortunately, there are also a number of adverse clinical effects associated with these broad-spectrum HDAC inhibitors which may raise further cautions in testing their potential therapeutic efficacy in PAH subjects. Clinical experience with non-specific HDAC inhibitors has been associated with electrocardiographic abnormalities and pulmonary embolism, both of which may have detrimental consequences in PAH patients.^{36, 37} Our current findings provide a number of key advancements in the role of MEF2, class IIa HDACs, and their targets in PAH that may facilitate the road to future translational studies: 1) We identify impairment of MEF2 activity in PAH PAECs that leads to decreased expression of a number of genes involved in vascular homeostasis; 2) We demonstrate that in addition to the epigenetic modifications achieved by HDAC inhibition and their potential roles in PAH, HDAC inhibitor mediated alteration of the protein-protein interactions may be a key unexplored mechanism by which these agents can impact pulmonary vascular remodeling; 3) We provide evidence that selective HDAC IIa inhibition can avoid the deterioration of RV function seen with broad spectrum HDAC inhibition, which would be detrimental in PAH patients. The MEF2 transcriptional targets we identified include: connexins 37 and 40, key gap junction proteins that may regulate vascular resistance and RV function,^{38,39} KLF2, whose overexpression in the lungs can improve RVSP in experimental PH models,⁴⁰ and miR-424 and 503, which were found to be significantly decreased in both PAH subject lungs as well as experimental models,^{8, 41} and can rescue PH models when overexpressed in the lungs.⁸ With respect to HDAC binding partners, the current study focused on the role of its inhibition of MEF2 activity, but other interactors, such as PPAR- γ ,⁴² may also be important in PAH, and deserve further investigation.^{24, 25, 43} The RV response to elevated pulmonary arterial pressures remains poorly understood, and is the subject of active investigation.⁴⁴ Our findings demonstrate that selective HDAC IIa inhibition does not induce RV fibrosis nor coronary artery endothelial apoptosis (as was seen with non-selective HDAC inhibition), and protected against RV dilatation. Investigation into the potential direct myocardial effect of HDAC IIa inhibition may demonstrate additional beneficial mechanisms above and beyond the decrease in pulmonary vascular resistance.

Although the PAECs used in this study were isolated from lungs of controls and PAH subjects and maintained expression of endothelial markers (data not shown), a potential limitation is whether their full endothelial phenotype is retained in culture and after passaging. The endothelial MEF2 targets included in this study represent those that are either validated MEF2 targets, including KLF2 and KLF4, as well as others we have confirmed to be targeted by the apelin-MEF2 axis both in vivo and in vitro.¹⁹ Identification and further validation of endothelial MEF2 transcriptional targets are areas of active investigation, and will shed further insights into its role in the pulmonary vasculature in the near future.

Overall, these findings define a novel signaling paradigm that may be critically important as we pursue new treatment strategies in PAH, while minimizing the adverse effects.

Additionally, the translation of these findings to clinical trials will likely be facilitated by the recent development of multiple promising HDAC IIa selective inhibitors,^{45–48} where therapeutic efficacy in PAH can be rapidly tested using the methodologies described here.

Supplementary Material

Refer to Web version on PubMed Central for supplementary material.

Acknowledgments

We thank P. Yu for critical reading of this manuscript, L. Peterson for assistance with the patient clinical information, and M. Aldred for providing the patient RNA samples.

Funding Sources: This study was supported by grants from the US National Institutes of Health (HL095654 and HL113005 to H.J.C. and HL60917 and HL115008 to S.C.E.), the Howard Hughes Medical Institute (Physician Scientist Early Career Award to H.J.C.), the American Heart Association (Established Investigator Award to H.J.C.), the National Research Foundation of Korea (Basic Science Research Program 2013R1A1A1057591 to J.K.), and the Korea Health Technology R&D Project through the Korea Health Industry Development Institute (KHIDI), funded by the Ministry of Health & Welfare, Republic of Korea (HI13C1372 to J.K.)

References

1. Rabinovitch M. Molecular pathogenesis of pulmonary arterial hypertension. *J Clin Invest.* 2012; 122:4306–4313. [PubMed: 23202738]
2. Grant JS, White K, MacLean MR, Baker AH. MicroRNAs in pulmonary arterial remodeling. *Cell Mol Life Sci.* 2013; 70:4479–4494. [PubMed: 23739951]
3. Humbert M, Sitbon O, Chaouat A, Bertocchi M, Habib G, Gressin V, Yaici A, Weitzenblum E, Cordier JF, Chabot F, Dromer C, Pison C, Reynaud-Gaubert M, Haloun A, Laurent M, Hachulla E, Cottin V, Degano B, Jais X, Montani D, Souza R, Simonneau G. Survival in patients with idiopathic, familial, and anorexigen-associated pulmonary arterial hypertension in the modern management era. *Circulation.* 2010; 122:156–163. [PubMed: 20585011]
4. Tuder RM, Groves B, Badesch DB, Voelkel NF. Exuberant endothelial cell growth and elements of inflammation are present in plexiform lesions of pulmonary hypertension. *Am J Pathol.* 1994; 144:275–285. [PubMed: 7508683]
5. Ricard N, Tu L, Le Hires M, Huertas A, Phan C, Thuillet R, Sattler C, Fadel E, Seferian A, Montani D, Dorfmueller P, Humbert M, Guignabert C. Increased pericyte coverage mediated by endothelial-derived fibroblast growth factor-2 and interleukin-6 is a source of smooth muscle-like cells in pulmonary hypertension. *Circulation.* 2014; 129:1586–1597. [PubMed: 24481949]
6. Izikki M, Guignabert C, Fadel E, Humbert M, Tu L, Zadigue P, Darteville P, Simonneau G, Adnot S, Maitre B, Raffestin B, Eddahibi S. Endothelial-derived fgf2 contributes to the progression of pulmonary hypertension in humans and rodents. *J Clin Invest.* 2009; 119:512–523. [PubMed: 19197140]
7. Dewachter L, Adnot S, Fadel E, Humbert M, Maitre B, Barlier-Mur AM, Simonneau G, Hamon M, Naeije R, Eddahibi S. Angiotensin/tie2 pathway influences smooth muscle hyperplasia in idiopathic pulmonary hypertension. *Am J Respir Crit Care Med.* 2006; 174:1025–1033. [PubMed: 16917117]
8. Kim J, Kang Y, Kojima Y, Lighthouse JK, Hu X, Aldred MA, McLean DL, Park H, Comhair SA, Greif DM, Erzurum SC, Chun HJ. An endothelial apelin-fgf link mediated by mir-424 and mir-503 is disrupted in pulmonary arterial hypertension. *Nat Med.* 2013; 19:74–82. [PubMed: 23263626]
9. Bogaard HJ, Mizuno S, Hussaini AA, Toldo S, Abbate A, Kraskauskas D, Kasper M, Natarajan R, Voelkel NF. Suppression of histone deacetylases worsens right ventricular dysfunction after pulmonary artery banding in rats. *Am J Respir Crit Care Med.* 2011; 183:1402–1410. [PubMed: 21297075]
10. Cavaasin MA, Demos-Davies K, Horn TR, Walker LA, Lemon DD, Birdsey N, Weiser-Evans MC, Harral J, Irwin DC, Anwar A, Yeager ME, Li M, Watson PA, Nemenoff RA, Buttrick PM,

- Stenmark KR, McKinsey TA. Selective class i histone deacetylase inhibition suppresses hypoxia-induced cardiopulmonary remodeling through an antiproliferative mechanism. *Circ Res.* 2012; 110:739–748. [PubMed: 22282194]
11. Bogaard HJ, Mizuno S, Voelkel NF. Letter by bogaard et al regarding article, “histone deacetylation inhibition in pulmonary hypertension: Therapeutic potential of valproic acid and suberoylanilide hydroxamic acid”. *Circulation.* 2013; 127:e539. [PubMed: 23569123]
 12. Zhao L, Chen CN, Hajji N, Oliver E, Cotroneo E, Wharton J, Wang D, Li M, McKinsey TA, Stenmark KR, Wilkins MR. Histone deacetylation inhibition in pulmonary hypertension: Therapeutic potential of valproic acid and suberoylanilide hydroxamic acid. *Circulation.* 2012; 126:455–467. [PubMed: 22711276]
 13. De Raaf MA, Hussaini AA, Gomez-Arroyo J, Kraskaukas D, Farkas D, Happe C, Voelkel NF, Bogaard HJ. Histone deacetylase inhibition with trichostatin a does not reverse severe angioproliferative pulmonary hypertension in rats (2013 grover conference series). *Pulm Circ.* 2014; 4:237–243. [PubMed: 25006442]
 14. Comhair SA, Xu W, Mavrakis L, Aldred MA, Asosingh K, Erzurum SC. Human primary lung endothelial cells in culture. *Am J Respir Cell Mol Biol.* 2012; 46:723–730. [PubMed: 22427538]
 15. Masri FA, Xu W, Comhair SA, Asosingh K, Koo M, Vasanthi A, Drazba J, Anand-Apte B, Erzurum SC. Hyperproliferative apoptosis-resistant endothelial cells in idiopathic pulmonary arterial hypertension. *Am J Physiol Lung Cell Mol Physiol.* 2007; 293:L548–554. [PubMed: 17526595]
 16. Sen-Banerjee S, Mir S, Lin Z, Hamik A, Atkins GB, Das H, Banerjee P, Kumar A, Jain MK. Kruppel-like factor 2 as a novel mediator of statin effects in endothelial cells. *Circulation.* 2005; 112:720–726. [PubMed: 16043642]
 17. Lu J, McKinsey TA, Nicol RL, Olson EN. Signal-dependent activation of the mef2 transcription factor by dissociation from histone deacetylases. *Proc Natl Acad Sci U S A.* 2000; 97:4070–4075. [PubMed: 10737771]
 18. Zhang CL, McKinsey TA, Chang S, Antos CL, Hill JA, Olson EN. Class ii histone deacetylases act as signal-responsive repressors of cardiac hypertrophy. *Cell.* 2002; 110:479–488. [PubMed: 12202037]
 19. Kang Y, Kim J, Anderson JP, Wu J, Gleim SR, Kundu RK, McLean DL, Kim JD, Park H, Jin SW, Hwa J, Quertermous T, Chun HJ. Apelin-apj signaling is a critical regulator of endothelial mef2 activation in cardiovascular development. *Circ Res.* 2013; 113:22–31. [PubMed: 23603510]
 20. Wang AH, Kruhlak MJ, Wu J, Bertos NR, Vezmar M, Posner BI, Bazett-Jones DP, Yang XJ. Regulation of histone deacetylase 4 by binding of 14-3-3 proteins. *Mol Cell Biol.* 2000; 20:6904–6912. [PubMed: 10958686]
 21. Grozinger CM, Schreiber SL. Regulation of histone deacetylase 4 and 5 and transcriptional activity by 14-3-3-dependent cellular localization. *Proc Natl Acad Sci U S A.* 2000; 97:7835–7840. [PubMed: 10869435]
 22. Fleming CL, Ashton TD, Gaur V, McGee SL, Pfeffer FM. Improved synthesis and structural reassignment of mc1568: A class iia selective hdac inhibitor. *J Med Chem.* 2014; 57:1132–1135. [PubMed: 24450497]
 23. Scognamiglio A, Nebbioso A, Manzo F, Valente S, Mai A, Altucci L. Hdac-class ii specific inhibition involves hdac proteasome-dependent degradation mediated by ranbp2. *Biochim Biophys Acta.* 2008; 1783:2030–2038. [PubMed: 18691615]
 24. Alastalo TP, Li M, de Perez VJ, Pham D, Sawada H, Wang JK, Koskenvuo M, Wang L, Freeman BA, Chang HY, Rabinovitch M. Disruption of ppargamma/beta-catenin-mediated regulation of apelin impairs bmp-induced mouse and human pulmonary arterial ec survival. *J Clin Invest.* 2011; 121:3735–3746. [PubMed: 21821917]
 25. Spiekerkoetter E, Tian X, Cai J, Hopper RK, Sudheendra D, Li CG, El-Bizri N, Sawada H, Haghghat R, Chan R, Haghghat L, de Jesus Perez V, Wang L, Reddy S, Zhao M, Bernstein D, Solow-Cordero DE, Beachy PA, Wandless TJ, Ten Dijke P, Rabinovitch M. Fk506 activates bmpr2, rescues endothelial dysfunction, and reverses pulmonary hypertension. *J Clin Invest.* 2013; 123:3600–3613. [PubMed: 23867624]
 26. Falcao-Pires I, Goncalves N, Henriques-Coelho T, Moreira-Goncalves D, Roncon-Albuquerque R Jr, Leite-Moreira AF. Apelin decreases myocardial injury and improves right ventricular function

- in monocrotaline-induced pulmonary hypertension. *Am J Physiol Heart Circ Physiol.* 2009; 296:H2007–2014. [PubMed: 19346461]
27. Chandra SM, Razavi H, Kim J, Agrawal R, Kundu RK, de Jesus Perez V, Zamanian RT, Quertermous T, Chun HJ. Disruption of the apelin-apj system worsens hypoxia-induced pulmonary hypertension. *Arterioscler Thromb Vasc Biol.* 2011; 31:814–820. [PubMed: 21233449]
 28. De Val S, Anderson JP, Heidt AB, Khiem D, Xu SM, Black BL. Mef2c is activated directly by ets transcription factors through an evolutionarily conserved endothelial cell-specific enhancer. *Dev Biol.* 2004; 275:424–434. [PubMed: 15501228]
 29. Subramanian SV, Nadal-Ginard B. Early expression of the different isoforms of the myocyte enhancer factor-2 (mef2) protein in myogenic as well as non-myogenic cell lineages during mouse embryogenesis. *Mech Dev.* 1996; 57:103–112. [PubMed: 8817457]
 30. Naya FJ, Black BL, Wu H, Bassel-Duby R, Richardson JA, Hill JA, Olson EN. Mitochondrial deficiency and cardiac sudden death in mice lacking the mef2a transcription factor. *Nat Med.* 2002; 8:1303–1309. [PubMed: 12379849]
 31. Lin Q, Schwarz J, Bucana C, Olson EN. Control of mouse cardiac morphogenesis and myogenesis by transcription factor mef2c. *Science.* 1997; 276:1404–1407. [PubMed: 9162005]
 32. Xu Z, Gong J, Maiti D, Vong L, Wu L, Schwarz JJ, Duh EJ. Mef2c ablation in endothelial cells reduces retinal vessel loss and suppresses pathologic retinal neovascularization in oxygen-induced retinopathy. *Am J Pathol.* 2012; 180:2548–2560. [PubMed: 22521302]
 33. Benisty JI, McLaughlin VV, Landzberg MJ, Rich JD, Newburger JW, Rich S, Folkman J. Elevated basic fibroblast growth factor levels in patients with pulmonary arterial hypertension. *Chest.* 2004; 126:1255–1261. [PubMed: 15486390]
 34. Li M, Riddle SR, Frid MG, El Kasmi KC, McKinsey TA, Sokol RJ, Strassheim D, Meyrick B, Yeager ME, Flockton AR, McKeon BA, Lemon DD, Horn TR, Anwar A, Barajas C, Stenmark KR. Emergence of fibroblasts with a proinflammatory epigenetically altered phenotype in severe hypoxic pulmonary hypertension. *J Immunol.* 2011; 187:2711–2722. [PubMed: 21813768]
 35. West AC, Johnstone RW. New and emerging hdac inhibitors for cancer treatment. *J Clin Invest.* 2014; 124:30–39. [PubMed: 24382387]
 36. Whittaker SJ, Demierre MF, Kim EJ, Rook AH, Lerner A, Duvic M, Scarisbrick J, Reddy S, Robak T, Becker JC, Samtsov A, McCulloch W, Kim YH. Final results from a multicenter, international, pivotal study of romidepsin in refractory cutaneous t-cell lymphoma. *J Clin Oncol.* 2010; 28:4485–4491. [PubMed: 20697094]
 37. Olsen EA, Kim YH, Kuzel TM, Pacheco TR, Foss FM, Parker S, Frankel SR, Chen C, Ricker JL, Arduino JM, Duvic M. Phase iib multicenter trial of vorinostat in patients with persistent, progressive, or treatment refractory cutaneous t-cell lymphoma. *J Clin Oncol.* 2007; 25:3109–3115. [PubMed: 17577020]
 38. Koval M, Billaud M, Straub AC, Johnstone SR, Zarbock A, Duling BR, Isakson BE. Spontaneous lung dysfunction and fibrosis in mice lacking connexin 40 and endothelial cell connexin 43. *Am J Pathol.* 2011; 178:2536–2546. [PubMed: 21641379]
 39. Johnson JA, West J, Maynard KB, Hemnes AR. Ace2 improves right ventricular function in a pressure overload model. *PLoS One.* 2011; 6:e20828. [PubMed: 21695173]
 40. Dungey AA, Deng Y, Yin J, Rozowsky S, Stewart DJ. Krüppel-like transcription factor-2 preserves endothelial function and protects against pulmonary hypertension. *American Heart Association Scientific Sessions.* 2011
 41. Caruso P, MacLean MR, Khanin R, McClure J, Soon E, Southgate M, MacDonald RA, Greig JA, Robertson KE, Masson R, Denby L, Dempsey Y, Long L, Morrell NW, Baker AH. Dynamic changes in lung microrna profiles during the development of pulmonary hypertension due to chronic hypoxia and monocrotaline. *Arterioscler Thromb Vasc Biol.* 2010; 30:716–723. [PubMed: 20110569]
 42. Yang Y, Qin X, Liu S, Li J, Zhu X, Gao T, Wang X. Peroxisome proliferator-activated receptor gamma is inhibited by histone deacetylase 4 in cortical neurons under oxidative stress. *J Neurochem.* 2011; 118:429–439. [PubMed: 21605119]
 43. Hansmann G, Wagner RA, Schellong S, Perez VA, Urashima T, Wang L, Sheikh AY, Suen RS, Stewart DJ, Rabinovitch M. Pulmonary arterial hypertension is linked to insulin resistance and

- reversed by peroxisome proliferator-activated receptor-gamma activation. *Circulation*. 2007; 115:1275–1284. [PubMed: 17339547]
44. Ryan JJ, Archer SL. The right ventricle in pulmonary arterial hypertension: Disorders of metabolism, angiogenesis and adrenergic signaling in right ventricular failure. *Circ Res*. 2014; 115:176–188. [PubMed: 24951766]
45. Isaacs JT, Antony L, Dalrymple SL, Brennen WN, Gerber S, Hammers H, Wissing M, Kachhap S, Luo J, Xing L, Bjork P, Olsson A, Bjork A, Leanderson T. Tasquinimod is an allosteric modulator of hdac4 survival signaling within the compromised cancer microenvironment. *Cancer Res*. 2013; 73:1386–1399. [PubMed: 23149916]
46. Lobera M, Madauss KP, Pohlhaus DT, Wright QG, Trocha M, Schmidt DR, Baloglu E, Trump RP, Head MS, Hofmann GA, Murray-Thompson M, Schwartz B, Chakravorty S, Wu Z, Mander PK, Kruidenier L, Reid RA, Burkhart W, Turunen BJ, Rong JX, Wagner C, Moyer MB, Wells C, Hong X, Moore JT, Williams JD, Soler D, Ghosh S, Nolan MA. Selective class iia histone deacetylase inhibition via a nonchelating zinc-binding group. *Nat Chem Biol*. 2013; 9:319–325. [PubMed: 23524983]
47. Muraglia E, Altamura S, Branca D, Cecchetti O, Ferrigno F, Orsale MV, Palumbi MC, Rowley M, Scarpelli R, Steinkuhler C, Jones P. 2-trifluoroacetylthiophene oxadiazoles as potent and selective class ii human histone deacetylase inhibitors. *Bioorg Med Chem Lett*. 2008; 18:6083–6087. [PubMed: 18930398]
48. Burli RW, Luckhurst CA, Aziz O, Matthews KL, Yates D, Lyons KA, Beconi M, McAllister G, Breccia P, Stott AJ, Penrose SD, Wall M, Lamers M, Leonard P, Muller I, Richardson CM, Jarvis R, Stones L, Hughes S, Wishart G, Haughan AF, O'Connell C, Mead T, McNeil H, Vann J, Mangette J, Maillard M, Beaumont V, Munoz-Sanjuan I, Dominguez C. Design, synthesis, and biological evaluation of potent and selective class iia histone deacetylase (hdac) inhibitors as a potential therapy for huntington's disease. *J Med Chem*. 2013; 56:9934–9954. [PubMed: 24261862]

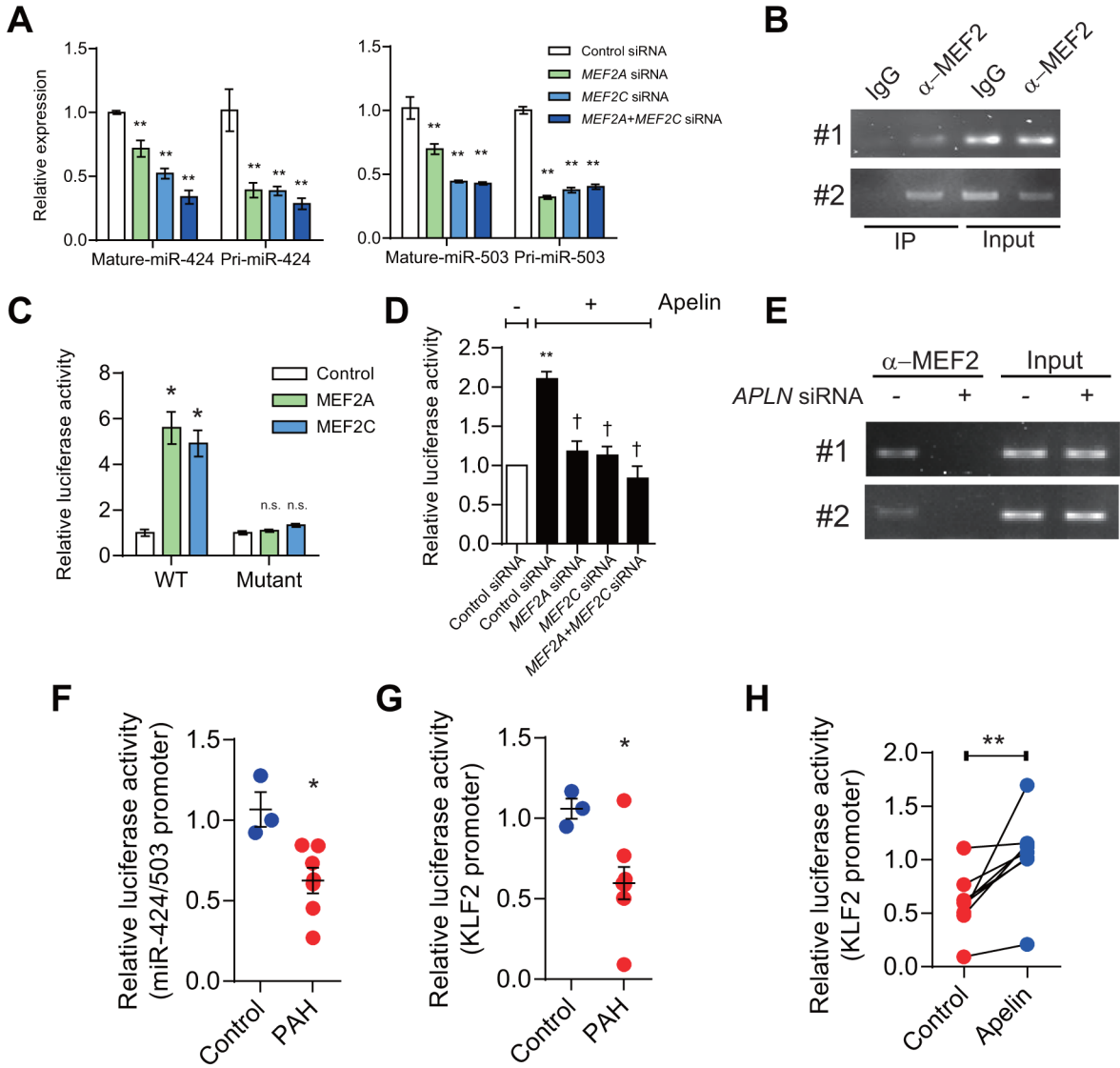
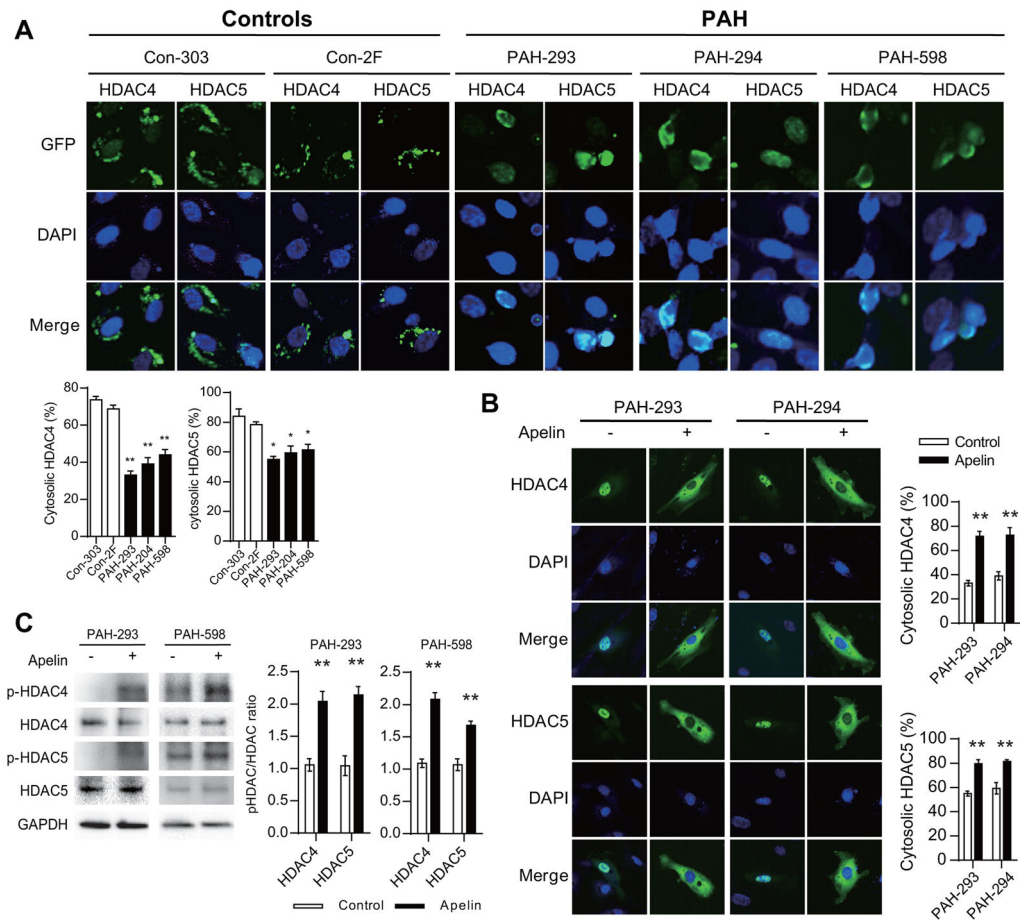


Figure 1. MEF2 activity is impaired in PAH PAECs. (A) Expression levels of the mature and the pri-forms of miR-424 and miR-503 in pulmonary artery endothelial cells (PAECs) in response to siRNA mediated knockdown of *MEF2A*, *MEF2C*, or both. ** $P < 0.01$ vs. control siRNA. (B) Chromatin immunoprecipitation (ChIP) assay using antibody against MEF2 or IgG control antibody in pull-down of the two MEF2 binding sites from the miR-424/503 promoter region. The immunoprecipitation (IP) and the input samples are shown. #1 and #2 represent the two putative MEF2 binding sites in the promoter of miR-424/503 (Sup. Fig. 1). (C) Luciferase reporter assays using PAECs transfected with either the wildtype (WT) or mutant miR-424/503 promoter based luciferase reporter in conjunction with MEF2A or MEF2C expression constructs. * $P < 0.05$ vs. control, n.s.: not significant. (D) Luciferase reporter assays using PAECs transfected with miR-424/503 promoter luciferase reporter in conjunction with apelin stimulation (1 μ M for 24 h) with concurrent knockdown of *MEF2A*, *MEF2C*, or both. ** $P < 0.01$ vs. unstimulated, † $P < 0.01$ vs. apelin stimulated with control

siRNA. **(E)** ChIP assay to determine MEF2 binding to the two predicted MEF2 binding sites in the miR-424/503 promoter using antibody against MEF2 in PAECs subjected to *APLN* knockdown. #1 and #2 represent the two putative MEF2 binding sites in the promoter of miR-424/503 (Sup. Fig. 1). **(F)** Luciferase reporter activity driven by the miR-424/503 promoter using control and PAH PAECs. * $P < 0.05$ vs. control PAECs. **(G)** Luciferase reporters driven by the KLF2 promoter region using control and PAH PAECs. * $P < 0.05$ vs. control PAECs. **(H)** KLF2 promoter driven luciferase reporter assay in PAH PAECs with apelin stimulation (1 μ M for 24 h). ** $P < 0.01$ vs. control.

**Figure 2.**

Dysregulated HDAC4 and HDAC5 in PAH PAECs. **(A)** Intracellular localization of transfected GFP tagged HDAC4 or HDAC5 (green) in control (Con) and PAH PAECs. DAPI (4',6-diamidino-2-phenylindole) nuclear stain is also shown (blue). ** $P < 0.01$ vs. Con-303, * $P < 0.05$ vs. Con-303. **(B)** HDAC4-GFP or HDAC5-GFP intracellular localization in response to apelin stimulation (1 μ M for 1 h) in PAH PAECs. ** $P < 0.01$ vs. control. **(C)** Phosphorylation of endogenously expressed HDAC4 and HDAC5 in response to apelin stimulation (1 μ M for 1 h) in PAH PAECs. ** $P < 0.01$ vs. unstimulated controls.

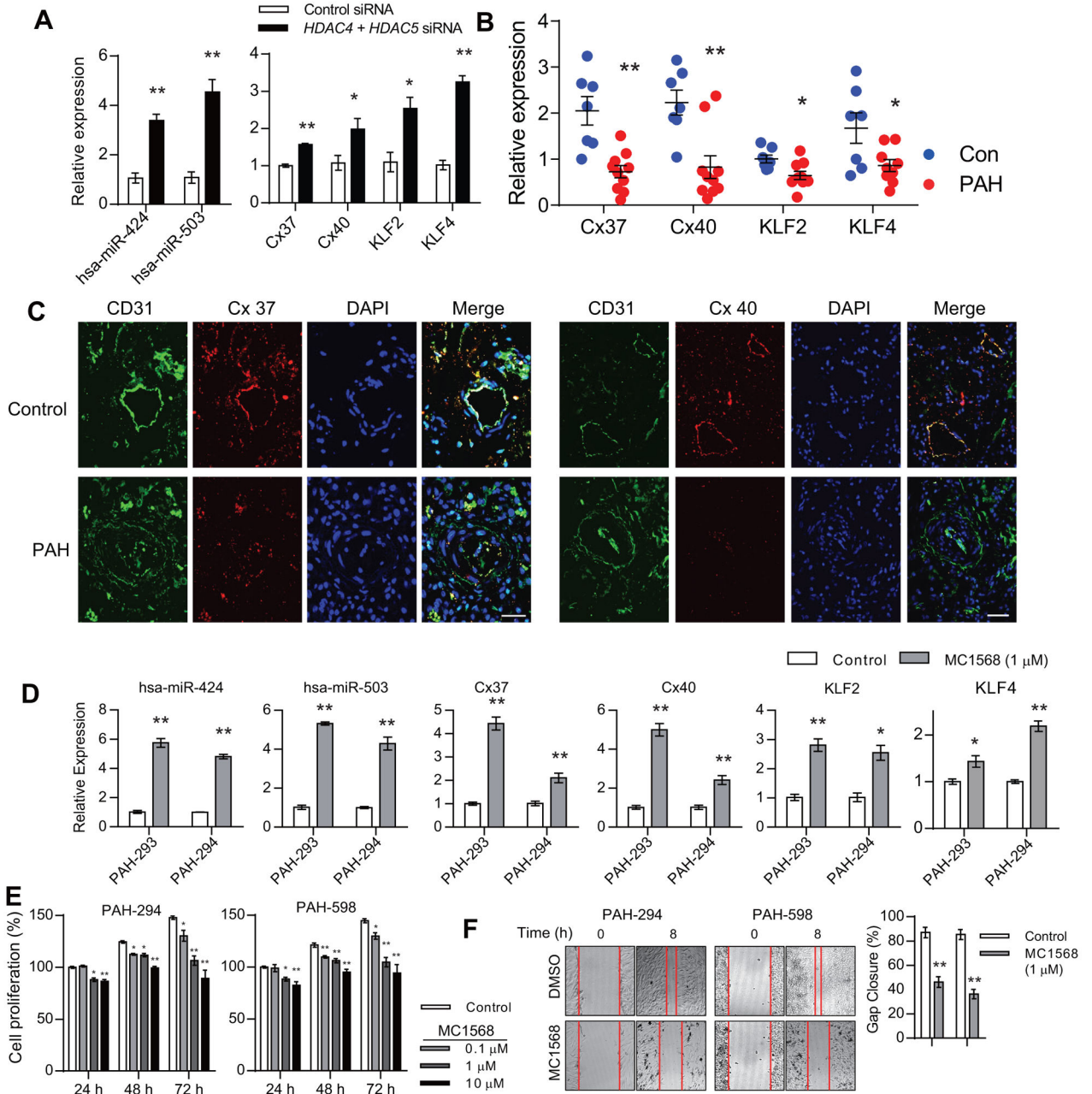
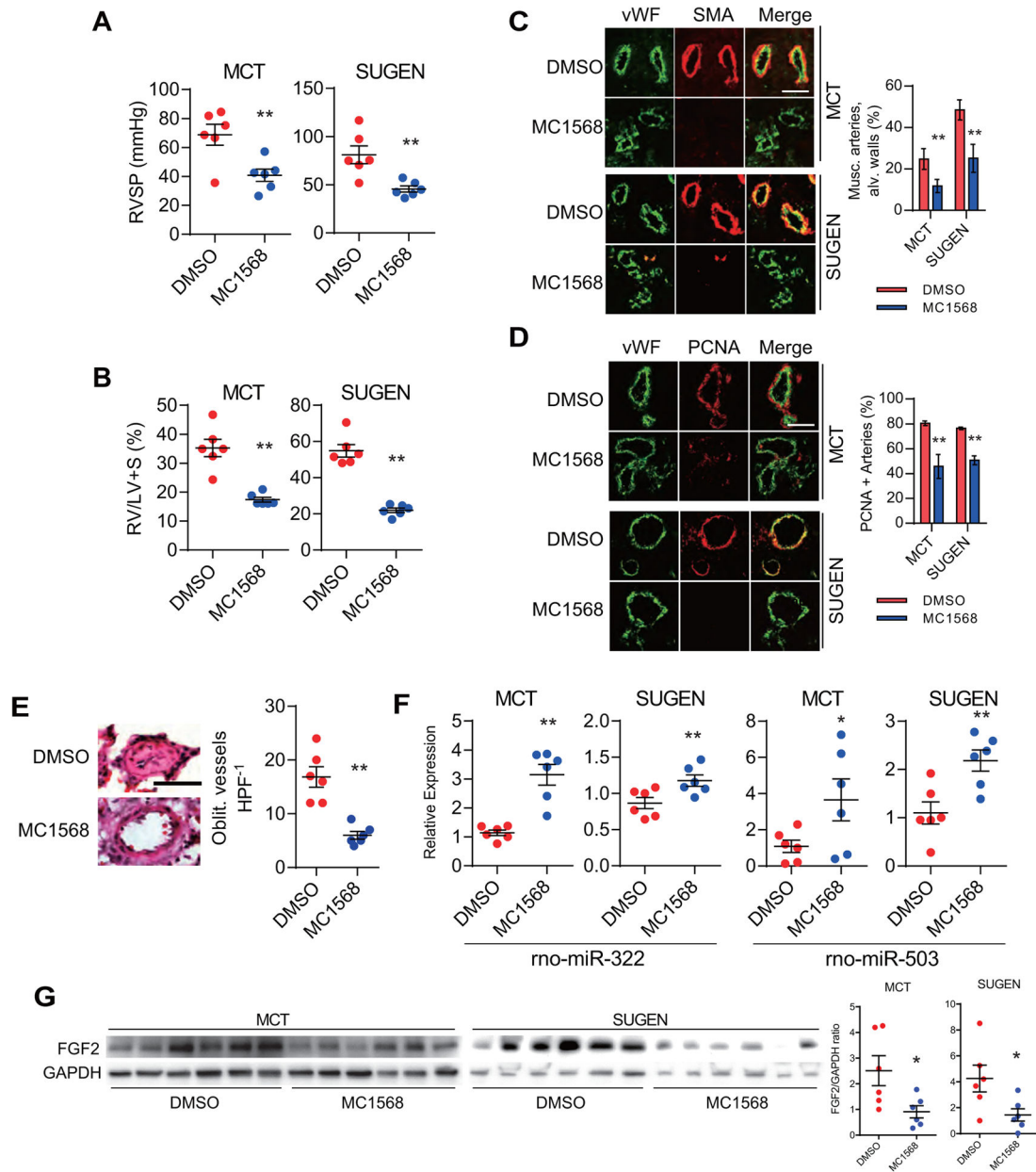


Figure 3. Selective inhibition of class IIa histone deacetylases (HDACs) restore pulmonary endothelial homeostasis. (A) Expression of hsa-miR-424, hsa-miR-503, connexin 37 (Cx37), connexin 40 (Cx40), KLF2 and KLF4 in response to knockdown of *HDAC4* and *HDAC5* in PAH PAECs. * $P < 0.05$ and ** $P < 0.01$ vs. control siRNA. (B) Transcript levels of Cx37, Cx40, KLF2 and KLF4 in PAECs from controls and PAH patients. * $P < 0.05$ and ** $P < 0.01$ vs. control PAECs. (C) Expression of Cx37 and Cx40 in lungs from control and PAH subject. CD31 is shown in green, connexin 37 and 40 are shown in red, DAPI nuclear staining is shown in blue. (D) Expression of hsa-miR-424, hsa-miR-503, Cx37, Cx40, KLF2

and KLF4 in PAH PAECs treated with MC1568 (1 μ M for 24 h). * P <0.05 and ** P <0.01 vs. control. Scale bar: 35 μ m. **(D)** Proliferation of PAH PAECs in response to MC1568 stimulation. * P <0.05 and ** P <0.01 vs. control. **(E)** PAH PAEC migration in response to MC1568 stimulation. ** P <0.01 vs. control.

**Figure 4.**

MC1568 rescues experimental models of pulmonary hypertension. (A) Right ventricular systolic pressure (RVSP) measurement in rats receiving either vehicle (DMSO) or MC1568 in the monocrotaline (MCT) and SU-5416/hypoxia (SUGEN) models. n=6 per group. ** $P < 0.01$ vs. vehicle treated rats. (B) Right ventricle to left ventricle + septum (RV/LV+S) weight ratios in the MCT and SUGEN models with either vehicle (DMSO) or MC1568 treatment. ** $P < 0.01$ vs. vehicle treated rats. (C) Muscularization (musc.) analysis of the pulmonary arterioles in the alveolar (alv.) wall of lungs from rats receiving either vehicle (DMSO) or MC1568 in the two experimental PH models. Smooth-muscle actin (SMA) is shown in red, and von Willebrand Factor (vWF) is shown in green. ** $P < 0.01$ vs. vehicle

treated rats in each model. Scale bar: 50 μm . **(D)** PCNA expression in the lungs of the two models receiving either vehicle (DMSO) or MC1568. PCNA is shown in red and vWF is shown in green. $**P < 0.01$ vs. vehicle treated rats in each model. Scale bar: 50 μm . **(E)** H&E staining of the lungs from rats subjected to SUGEN pulmonary hypertension induction receiving either DMSO or MC1568. The average number of obliterated vessels per microscopic field (Oblit. vessels HPF¹) is shown. $**P < 0.01$ vs. vehicle treated rats. Scale bar: 25 μm . **(F)** Expression levels of rno-miR-322 (the rat homolog of hsa-miR-424) and rno-miR-503 in the rat lungs of the PH models with either vehicle (DMSO) or MC1568 treatment. $*P < 0.05$ and $**P < 0.01$ vs. vehicle treated rats. **(G)** FGF2 protein expression in lung homogenates of rats in the two PH models in response to MC1568 treatment. The graph represents FGF2/GAPDH intensity ratio. $*P < 0.05$.

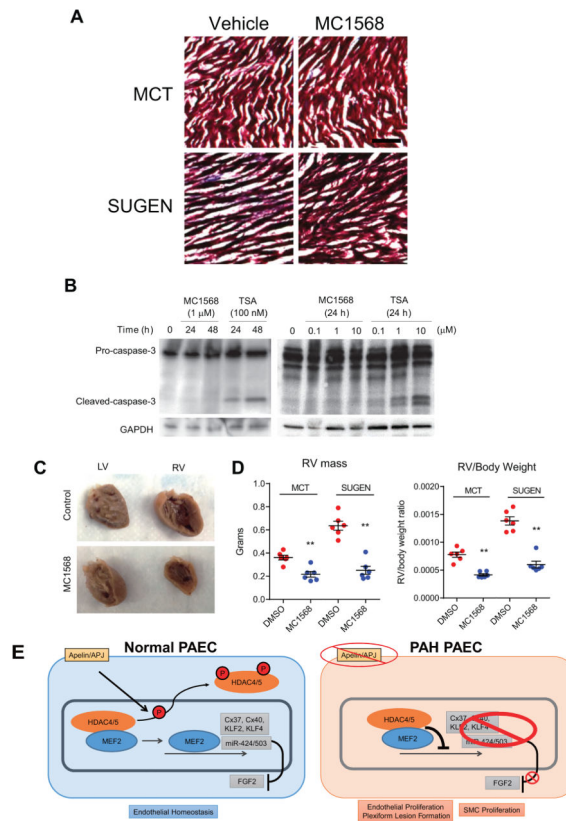


Figure 5. Class IIa HDAC inhibition does not promote RV fibrosis or coronary artery endothelial cell apoptosis. **(A)** Trichrome stain of the right ventricle from the four treatment groups. Scale bar: 100 mm. **(B)** Effects of MC1568 or trichostatin A (TSA) on caspase 3 cleavage in human coronary artery endothelial cells. **(C)** Gross appearance of LV and RV in the hearts of the SUGEN PH model in the DMSO (control) and MC1568 groups. **(D)** RV weights and the RV to total body weight ratio of rats in the four groups of animals. ** $P < 0.01$ vs. DMSO (control) in each group. **(E)** Working model of the signaling cascade.